Direction-of-Arrival Estimation using a Low-Complexity Covariance-Based Approach

TADEU N. FERREIRA, Member, IEEE
Fluminense Federal University

SERGIO L. NETTO, Senior Member, IEEE
PAULO S. R. DINIZ, Fellow, IEEE
Federal University of Rio de Janeiro

This article presents a new algorithm for performing direction-of-arrival (DOA) estimation using manipulations on covariance matrices. The proposed algorithm combines a new formulation for data projection on real subspaces, together with beamspace decompositions, reducing the sizes of all data structures and computational complexity of the resulting estimation process. Theoretical analyses as well as computer simulations indicate that the proposed algorithm reduces its ESPRIT equivalent computational complexity by a minimum of 20%, while presenting similar mean-square error (MSE) performance.

Manuscript received February 28, 2011; released for publication May 24, 2011.

IEEE Log No. T-AES/48/3/943994.

Refereeing of this contribution was handled by J. Taque.

This work was supported by CNPq and FAPERJ.

Authors' addresses: T. N. Ferreira, Telecommunications Engineering Department, Fluminense Federal University, Rua Passo da Pátria, 156, Bloco D-Sala 504, Niterói, RJ 24210-240, Brazil, E-mail: (tadeu_zito@gmail.com); T. N. Ferreira, S. L. Netto, and P. S. R. Diniz, Electrical Engineering Program, Federal University of Rio de Janeiro (UFRJ), Rio de Janeiro, Brazil.

I. INTRODUCTION

In the uplink connection of a wireless communication system, the use of an antenna array in the receiver provides some advantages in comparison to the traditional single-antenna receiver, such as increasing channel capacity and spectrum efficiency [1]. In wireless communications, systems providing source localization may be used to spatially separate information of the desired users from interference.

If the source positions are approximately co-planar in the far-field of the receiving array, the medium is isotropic, and narrowband signals are transmitted, the source localization problem simplifies into the determination of the angle θ of arrival, as illustrated in Fig. 1, commonly referred to as a direction-of-arrival (DOA) estimation [2].

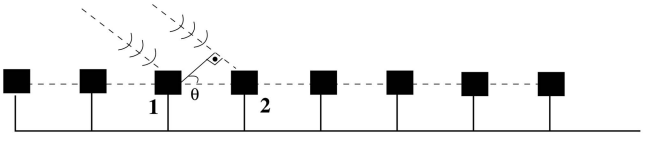

Fig. 1. Angle θ of arrival estimated by DOA estimation problem.

The first algorithms for this purpose estimated the entire received waveforms to extract the desired DOAs. In order to reduce the overall computational complexity of the estimation process, transmission was then remodeled and the DOA estimation was performed as a parametric problem, such as in the classic MUSIC (multiple signal classification) algorithm [3]. The original version of MUSIC, known as spectral MUSIC, requires an exhaustive search for the DOA estimation, which was very computationally intensive. In order to further reduce the algorithmic computational complexity, the ESPRIT (estimation of parameters via rotational invariance techniques) algorithm imposed some constraints on the receiving array geometry, thus allowing one to exploit redundancies in the resulting system representation [4]. The topic of reducing data dimensionality using subspace methods received renewed interest, as can be illustrated by a recent thematic issue of the *IEEE Signal Processing Magazine* on subspace-based reduced-rank algorithms [5].

This article presents a new DOA estimating algorithm developed with the covariance-based (CB) approach, which operates onto subpartitions of the data autocorrelation matrix, allied to the beamspace method, which projects received data into a subspace of reduced dimensions. This combination is based on a new formulation for the real-only-operation scheme, which reduces the complexity of arithmetic operations by avoiding data representation in the complex domain. The result is an entirely new algorithm with reduced computational complexity and equivalent estimation performance as compared with its ESPRIT

counterpart. Such characteristics are validated by both theoretical analysis and simulation results.

This paper is organized as follows. In Section II we present a detailed model for the DOA estimation problem, establishing the notation used throughout the remaining sections. Section III reviews the conception of the elementspace CB-DOA scheme, the beamspace projection, and discusses a new formulation for the real-only-operation approach. Insights are provided for each of these methods expliciting the algorithm simplifications achieved by each proposal. Section IV combines concepts from the three techniques seen in Section III to inspire a lower complexity scheme for DOA estimation. Theoretical mean-squared error (MSE) analyses and associated computational burden for the proposed algorithm are evaluated in Sections V and VI, respectively, in comparison to the corresponding ESPRIT version. Finally, Section VII includes simulations of the CB family of algorithms in different scenarios illustrating the MSE performance achieved by the proposed method.

II. STANDARD DOA ESTIMATION BASED ON ESPRIT

In this section the DOA estimation process is presented. In Section IIA, the environment for the DOA estimation is described, comprising M sources and N sensors with the constraints on the geometry of the array. Then, in Section IIB, standard ESPRIT algorithm for the DOA estimation is reviewed.

A. System Modeling

Consider a communication scenario with M transmitting sources and N sensors in the receiving array. By representing the mth transmitted signal belonging to the mth source as $s_m(k)$ and the ith sensor signal as $x_i(k)$, the transmission model may be written as

$$x_i(k) = \sum_{m=0}^{M-1} s_m(k) a_i(\theta_m) + n_i(k) \tag{1}$$

for $0 \leq i < N$, where $n_i(k)$ represents an additive white Gaussian noise (AWGN) realization for each receiving sensor and $a_i(\theta_m)$ denotes the gain of the ith antenna in the direction of the mth source.

By defining the data structures

$$\mathbf{s}(k) = [s_0(k) \quad s_1(k) \cdots s_{M-1}(k)]^{\mathrm{T}} \tag{2}$$

$$\mathbf{x}(k) = [x_0(k) \quad x_1(k) \cdots x_{N-1}(k)]^{\mathrm{T}} \tag{3}$$

$$\mathbf{n}(k) = [n_0(k) \quad n_1(k) \cdots n_{N-1}(k)]^{\mathrm{T}} \tag{4}$$

$$\mathbf{A} = \begin{bmatrix} a_0(\theta_0) & a_0(\theta_1) & \cdots & a_0(\theta_{M-1}) \\ a_1(\theta_0) & a_1(\theta_1) & \cdots & a_1(\theta_{M-1}) \\ \vdots & \vdots & \ddots & \vdots \\ a_{N-1}(\theta_0) & a_{N-1}(\theta_1) & \cdots & a_{N-1}(\theta_{M-1}) \end{bmatrix} \tag{5}$$

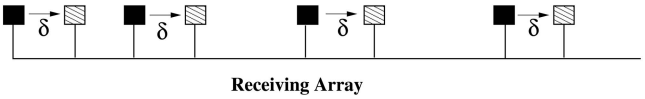

Fig. 2. Doublet division of receiving array with constant sensor displacement.

where matrix $\mathbf{A}$ is commonly referred to as the array manifold matrix, (1) may be rewritten as

$$\mathbf{x}(k) = \mathbf{A}\mathbf{s}(k) + \mathbf{n}(k). \tag{6}$$

The receiving array may be divided into subarrays with a constant displacement vector $\boldsymbol{\delta}$, one subarray comprising the initial points of the displacement vectors and the other containing the corresponding terminal points, as represented in Fig. 2. Any antenna may belong to two different doublets, since it may be the initial point of one displacement vector and also the terminal point of another one, generating overlapping subarrays.

The system model for the two receiving subarrays of length P then becomes

$$x_{0,i}(k) = \sum_{m=0}^{M-1} s_m(k) a_i(\theta_m) + n_{0,i}(k) \tag{7}$$

$$x_{1,i}(k) = \sum_{m=0}^{M-1} s_m(k) e^{(\mathrm{j}\omega\delta/c)\sin\theta_m} a_i(\theta_m) + n_{1,i}(k) \tag{8}$$

for $0 \leq i < P$, where ω denotes the signal carrier angular frequency and c stands for the speed of light.

B. ESPRIT Algorithm

By performing a generalized eigenvalue-eigenvector decomposition (GEVD) [7] on the pair of covariance matrices $\mathbf{R}_x = E[\mathbf{x}(k)\mathbf{x}^{\mathrm{H}}(k)]$ and $\mathbf{R}_n = E[\mathbf{n}(k)\mathbf{n}^{\mathrm{H}}(k)]$, one gets

$$\mathrm{GEVD}(\mathbf{R}_x, \mathbf{R}_n) = \mathbf{U}\boldsymbol{\Lambda}\mathbf{U}^{\mathrm{H}} \tag{9}$$

with $\boldsymbol{\Lambda} = \mathrm{diag}(\lambda_0, \lambda_1, \ldots, \lambda_{N-1})$ representing a diagonal matrix containing the generalized eigenvalue diagonal matrix. The generalized eigenvectors $\mathbf{e}_i$ associated to the M largest generalized eigenvalues of $\mathbf{R}_x$ may be then grouped to form the $N \times M$ matrix $\mathbf{U}_s$

$$\mathbf{U}_s = \mathbf{R}_n[\mathbf{e}_0 \quad \mathbf{e}_1 \cdots \mathbf{e}_{M-1}] \tag{10}$$

whose column subspace is the so-called signal subspace. Hence, one can show that there is a full-rank matrix $\mathbf{T}$ such that [4]

$$\mathbf{U}_s = \mathbf{A}\mathbf{T} \tag{11}$$

which presents an invariance in the signal subspace [4]

$$\mathbf{J}_0^{P,N}\mathbf{U}_s\boldsymbol{\Psi} = \mathbf{J}_1^{P,N}\mathbf{U}_s \tag{12}$$

where $\mathbf{\Psi}$ is a full-rank matrix and

$$\mathbf{J}_0^{a,b} = [\mathbf{I}_a \quad \mathbf{0}_{a\times(b-a)}] \tag{13}$$

$$\mathbf{J}_1^{a,b} = [\mathbf{0}_{a\times(b-a)} \quad \mathbf{I}_a] \tag{14}$$

are selection matrices. Finally, the eigenvalue/eigenvector decomposition (EVD) of $\mathbf{\Psi}$ yields

$$\mathbf{\Psi} = \mathbf{T}\mathbf{\Phi}\mathbf{T}^{-1} \tag{15}$$

where

$$\mathbf{\Phi} = \text{diag}(\phi_0, \phi_1, \ldots, \phi_{M-1}) \tag{16}$$

for $\phi_m = e^{(\text{j}\omega\delta/c)\sin\theta_m}$ and considering that operator diag(·) denotes a diagonal matrix whose entries are specified by the input parameters. The ESPRIT algorithm solves (12), using, for instance, a total least-squares (TLS) technique. TLS is used to determine $\mathbf{\Psi}$ and then obtain the diagonal parameter matrix $\mathbf{\Phi}$ through (15). The resulting DOA estimates are given by

$$\hat{\theta}_m = \arcsin\left(\frac{c}{\text{j}\omega\delta}\ln(\phi_m)\right) \qquad \text{for} \quad 0 \le m < M \tag{17}$$

where ln(·) denotes the natural logarithm function.

III. COVARIANCE-BASED DOA TECHNIQUES

In this section we revisit two CB-DOA estimation techniques: the elementspace CB-DOA approach presented in [6] and the discrete Fourier transform (DFT)-based beamspace CB-DOA [2, 11]. Besides that, we present an alternative formulation for the real CB-DOA. With this new formulation, the concepts underlying these three techniques inspire, as presented later in Section IV, the creation of a single algorithm that represents a low-complexity alternative to the ESPRIT algorithm.

A. Elementspace CB-DOA Algorithm

The received data autocovariance matrix $\mathbf{R}_x$ employed by the ESPRIT algorithm can be partitioned into four smaller submatrices. Data in those four submatrices present some redundancy. Therefore, we use two smaller covariance structures

$$\mathbf{R}_{x00} = \mathbf{J}_0^{P,N}\mathbf{R}_x(\mathbf{J}_0^{P,N})^{\text{T}} = \mathbf{A}_0\mathbf{R}_s\mathbf{A}_0^{\text{H}} + \mathbf{R}_{n00} \tag{18}$$

$$\mathbf{R}_{x01} = \mathbf{J}_0^{P,N}\mathbf{R}_x(\mathbf{J}_1^{P,N})^{\text{T}} = \mathbf{A}_0\mathbf{R}_s\mathbf{\Phi}\mathbf{A}_0^{\text{H}} + \mathbf{R}_{n01}. \tag{19}$$

Since $\mathbf{J}_0^{P,N}\mathbf{x}(k)$ represents data belonging to the first subarray, whereas $\mathbf{J}_1^{P,N}\mathbf{x}(k)$ contains data from the other subarray, (18) and (19), respectively, represent the autocovariance of the first subarray and a crosscovariance between the subarrays. By performing the GEVD on the pair $(\mathbf{R}_{x00}, \mathbf{R}_{n00})$, one may write [7]

$$\text{GEVD}(\mathbf{R}_{x00}, \mathbf{R}_{n00}) = \mathbf{U}\mathbf{\Lambda}\mathbf{U}^{\text{H}}. \tag{20}$$

The signal subspace can be estimated from the M largest generalized eigenvalues of $\mathbf{\Lambda}$ and their associated generalized eigenvectors, respectively comprising matrices $\mathbf{\Lambda}_s$ and $\mathbf{U}_s$. The CB-DOA algorithm proceeds by applying a similarity transformation $\mathbf{F} = (\mathbf{\Lambda}_s^{1/2})^{-1}\mathbf{U}_s^{\text{H}}$ on the matrix pencil $(\mathbf{R}_{x01} - \mathbf{R}_{n01})$ such that [6, 9]

$$\begin{aligned}\mathbf{\Psi} &= \mathbf{F}(\mathbf{R}_{x10} - \mathbf{R}_{n10})\mathbf{F}^{-1} \\ &= \mathbf{F}\mathbf{A}_0\mathbf{T}\mathbf{R}_s^{1/2}\mathbf{\Phi}(\mathbf{R}_s^{1/2})^{\text{H}}\mathbf{T}^H\mathbf{A}_0^{\text{H}}\mathbf{F}^{-1}\end{aligned} \tag{21}$$

where $\mathbf{T}$ is a full-rank matrix representing a rotational incertainty in the estimation of the column subspace. Therefore, as in the ESPRIT algorithm, the EVD of $\mathbf{\Psi}$ provides an estimate of $\mathbf{\Phi}$, which leads to the desired DOA estimates through (17). The elementspace CB-DOA algorithm represents a low-complexity alternative to ESPRIT, since it is based on matrices of reduced dimensions.

B. Beamspace CB-DOA Algorithm

Beamspace processing is a well-known technique [2, 10] which projects the received data on a subspace of reduced dimensions. Such projections, however, may affect the rotational invariance property of the signal subspace, generated by the geometric constraints depicted in Fig. 2, of the elementspace versions of either the ESPRIT or CB-DOA algorithms. Additional processing must then be performed on the receiving data to ensure proper algorithmic convergence.

By choosing the projection matrix $\mathbf{W}$ as the DFT matrix, the ith column is represented by

$$\mathbf{w}_i = e^{(2\pi\text{j}m/N)((N-1)/2)}[1 \quad e^{-2\pi\text{j}m/N} \cdots e^{-2\pi\text{j}m(N-1)/N}]^{\text{T}}. \tag{22}$$

The received data $\mathbf{x}(k)$, as modeled in (6), can be projected onto the DFT beamspace through the operation

$$\mathbf{x}_b(k) = \begin{bmatrix}\mathbf{x}_{b,0}(k) \\ \mathbf{x}_{b,1}(k)\end{bmatrix} = \mathbf{W}_{L,b}^{\text{H}}\mathbf{x}(k) \qquad \text{for} \quad 0 \le b < B \tag{23}$$

where each $\mathbf{W}_{L,b}$ contains any L out of the N columns of $\mathbf{W}$. One may interpret the L columns of $\mathbf{W}$ as preselecting a subset of possible arriving directions, leading to a simplified DOA search in an L-dimensional angle subspace with $L \le N$.

If the first L rows and the last L rows of $\mathbf{W}_{L,b}$ span the same subspace, there must be an $L \times L$ full-rank matrix $\mathbf{B}$ such that

$$\mathbf{J}_0^{L,N}\mathbf{W}_{L,b} = \mathbf{J}_1^{L,N}\mathbf{W}_{L,b}\mathbf{B} \tag{24}$$

with $\mathbf{J}_0^{L,N}$ and $\mathbf{J}_1^{L,N}$ as defined in (13) and (14). Using the DFT beamspace projection, a redundancy in the

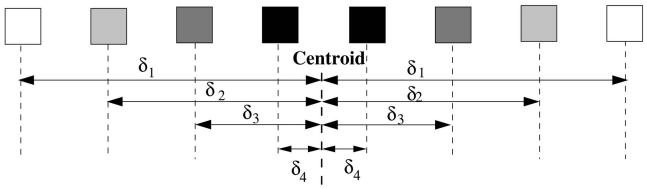

Fig. 3. Representation of a CH receiving array, with identical colors indicating the same directional gain.

signal subspace may be found by defining an $L \times L$ full-rank matrix $\mathbf{K}_b$ satisfying [11]

$$\mathbf{K}_b \mathbf{W}_{L,b}^{\mathrm{H}} \mathbf{U}_s = \mathbf{K}_b \mathbf{B}^{\mathrm{H}} \mathbf{W}_{L,b}^{\mathrm{H}} \mathbf{U}_s \boldsymbol{\Psi}^{\mathrm{H}} \tag{25}$$

where $\mathbf{U}_s = \mathbf{AT}$ spans the signal subspace of $\mathbf{R}_{x,b}$ and $\boldsymbol{\Psi}^{\mathrm{H}} = \mathbf{T}\boldsymbol{\Phi}^{\mathrm{H}}\mathbf{T}^{-1}$, as before. Equation (25) represents an invariance equation in the beamspace, which leads to the beamspace CB-DOA algorithm described in [11].

C. New Version for Real CB-DOA Algorithm

Some data projections may reduce the complexity of the resulting DOA algorithm by avoiding complex arithmetic operations at the price of more severe constraints in the antenna array geometry. A receiving array, which is symmetric with respect to antenna positioning and corresponding directional gains, as depicted in Fig. 3, is referred to as a centro-Hermitian (CH) array. This array configuration leads to an array manifold such that

$$\boldsymbol{\Pi}_N \mathbf{A}^* \boldsymbol{\Pi}_M = \mathbf{A} \tag{26}$$

where $\boldsymbol{\Pi}_N$ denotes an $N \times N$ permutation matrix with ones in its antidiagonal and zeros elsewhere and the superscript asterisk stands for the complex conjugate operation. Therefore, a CH array yields a system modeling with an array manifold possessing CH property which allows a subspace projection in which only real operations are required for estimating $\boldsymbol{\Phi}$, as described in [12].

In this subsection we introduce a new real CB-DOA algorithm which is compatible with the beamspace decomposition, allowing one to combine the two schemes, as explored in Section IV. This new real algorithm is based on a uniform linear array (ULA), that is, an array receiving sensors which is uniformly spaced in a line. In such a case, each column $\mathbf{a}_i$ in the array manifold matrix $\mathbf{A}$ becomes [13]

$$\mathbf{a}_i = \left\{\exp\left[-(\mathrm{j}\omega\delta/c)((N-1)/2)\sin\theta_i\right] \cdots \exp\left[-(\mathrm{j}\omega\delta/c)\sin\theta_i\right] 1 \cdots \exp\left[(\mathrm{j}\omega\delta/c)((N-1)/2)\sin\theta_i\right]\right\}^T \tag{27}$$

where the amount of sensors N is assumed to be odd. We also consider that the two receiving subarrays present maximal overlap, that is, the first sensor only belongs to the first subarray, the last sensor only belongs to the second subarray and all the other sensors take part in both subarrays. Under these conditions, the receiver subarrays become

$$\mathbf{x}_0(k) = \mathbf{J}_0^{N,1} \mathbf{x}(k) \tag{28}$$

$$\mathbf{x}_1(k) = \mathbf{J}_1^{N,1} \mathbf{x}(k). \tag{29}$$

Consider $\mathbf{Q}_{R,a}$, for odd-valued a, such that

$$\mathbf{Q}_{R,a} = \frac{1}{\sqrt{2}} \begin{bmatrix} \mathbf{I}_{(a-1)/2} & 0 & \mathrm{j}\mathbf{I}_{(a-1)/2} \\ \mathbf{0}_{(a-1)/2\times 1}^{\mathrm{T}} & \sqrt{2} & \mathbf{0}_{(a-1)/2\times 1}^{\mathrm{T}} \\ \boldsymbol{\Pi}_{(a-1)/2} & 0 & -\mathrm{j}\boldsymbol{\Pi}_{(a-1)/2} \end{bmatrix}. \tag{30}$$

By grouping K data snapshots in a columnwise manner, we can define the auxiliary matrix

$$\mathbf{X} = [\mathbf{x}(0) \quad \mathbf{x}(1) \cdots \mathbf{x}(K-1)] \tag{31}$$

and the projection $\mathbf{Q}_{R,a}$ can be applied to $\mathbf{X}$ in a similar way as in the beamspace CB-DOA algorithm, leading to

$$\mathbf{X}_r = [\mathbf{x}_r(0) \quad \mathbf{x}_r(1) \cdots \mathbf{x}_r(K-1)] = \mathbf{Q}_{R,a}\mathbf{X}. \tag{32}$$

Consider matrix $\mathbf{X}_{RI}$ which uses the real and imaginary parts of $\mathbf{X}_r$, denoted by $\Re(\mathbf{X}_r)$ and $\Im(\mathbf{X}_r)$, respectively, as indicated by

$$\mathbf{X}_{RI} = [\Re(\mathbf{X}_r) \quad \Im(\mathbf{X}_r)] \begin{bmatrix} (\Re(\mathbf{X}_r^{\mathrm{T}})) \\ (\Im(\mathbf{X}_r^{\mathrm{T}})) \end{bmatrix}. \tag{33}$$

By applying the selection matrices

$$\mathbf{K}_0 = \mathbf{Q}_{R,N-1}^{\mathrm{H}} (\mathbf{J}_{0,N-1} + \boldsymbol{\Pi}_{N-1}\mathbf{J}_{0,N-1}\boldsymbol{\Pi}_N)\mathbf{Q}_{R,N} \tag{34}$$

$$\mathbf{K}_1 = \mathbf{Q}_{R,N-1}^{\mathrm{H}} (\mathbf{J}_{0,N-1} - \boldsymbol{\Pi}_{N-1}\mathbf{J}_{0,N-1}\boldsymbol{\Pi}_N)\mathbf{Q}_{R,N} \tag{35}$$

for subarray separation, the following new invariance equation arises

$$\mathbf{K}_0 \mathbf{Q}_{R,N}^{\mathrm{H}} \mathbf{A}\boldsymbol{\Omega} = \mathbf{K}_1 \mathbf{Q}_{R,N}^{\mathrm{H}} \mathbf{A} \tag{36}$$

where

$$\boldsymbol{\Omega} = \mathrm{diag}\left(\tan\frac{\omega\sin\theta_0}{2c}, \tan\frac{\omega\sin\theta_1}{2c}, \ldots, \tan\frac{\omega\sin\theta_{M-1}}{2c}\right). \tag{37}$$

IV. DFT-BEAMSPACE REAL CB-DOA ALGORITHM

The CB approach, beamspace projection, and real-only-operation techniques inspire a new algorithm with significant reduction both on the amount and on the size of all data structures employed by the resulting DOA estimating algorithm. In such context, consider the ULA receiver which leads to the array manifold matrix $\mathbf{A}$ whose columns $\mathbf{a}_i$ are given by (27) [13], where the amount of sensors N is assumed to be odd.

Consider also the data matrix $\mathbf{X}$ comprising K data snapshots in a columnwise manner, as in (31), which can be projected onto the DFT beamspace by applying the projection matrix $\mathbf{W}_{L,b}$ defined in (23), resulting in

$$\mathbf{Y}_r = \mathbf{W}_{L,b}^{\mathrm{H}} \mathbf{X}. \tag{38}$$

Hence, an auxiliary autocovariance structure $\mathbf{Y}_{RI}$ can be defined as

$$\mathbf{Y}_{RI} = [\Re(\mathbf{Y}_r) \quad \Im(\mathbf{Y}_r)] \begin{bmatrix} (\Re(\mathbf{Y}_r^{\mathrm{T}})) \\ (\Im(\mathbf{Y}_r^{\mathrm{T}})) \end{bmatrix} \tag{39}$$

where $\Re(\mathbf{Y}_r)$ and $\Im(\mathbf{Y}_r)$ denote the real and imaginary parts of $\mathbf{Y}_r$, respectively. This auxiliary structure leads to the following invariance equation [13]:

$$\mathbf{\Gamma}_0 \mathbf{W}_{L,b}^{\mathrm{H}} \mathbf{A} \mathbf{\Omega} = \mathbf{\Gamma}_1 \mathbf{W}_{L,b}^{\mathrm{H}} \mathbf{A} \tag{40}$$

where

$$\mathbf{\Gamma}_0 = \begin{bmatrix} 1 & \mathrm{c}\left(\frac{\pi}{N}\right) & 0 & \cdots & 0 & 0 \\ 0 & \mathrm{c}\left(\frac{\pi}{N}\right) & \mathrm{c}\left(\frac{2\pi}{N}\right) & \cdots & 0 & 0 \\ \vdots & \vdots & \vdots & \ddots & \vdots & \vdots \\ 0 & 0 & 0 & \cdots & \mathrm{c}\left((N-2)\frac{\pi}{N}\right) & \mathrm{c}\left((N-1)\frac{\pi}{N}\right) \\ (-1)^N & 0 & 0 & \cdots & 0 & \mathrm{c}\left((N-1)\frac{\pi}{N}\right) \end{bmatrix} \tag{41}$$

$$\mathbf{\Gamma}_1 = \begin{bmatrix} 0 & \mathrm{s}\left(\frac{\pi}{N}\right) & 0 & \cdots & 0 & 0 \\ 0 & \mathrm{s}\left(\frac{\pi}{N}\right) & \mathrm{s}\left(\frac{2\pi}{N}\right) & \cdots & 0 & 0 \\ \vdots & \vdots & \vdots & \ddots & \vdots & \vdots \\ 0 & 0 & 0 & \cdots & \mathrm{s}\left((N-2)\frac{\pi}{N}\right) & \mathrm{s}\left((N-1)\frac{\pi}{N}\right) \\ 0 & 0 & 0 & \cdots & 0 & \mathrm{s}\left((N-1)\frac{\pi}{N}\right) \end{bmatrix} \tag{42}$$

where $\mathrm{c}(\cdot)$ and $\mathrm{s}(\cdot)$, respectively, stand for the cosine and sine functions.

Consider now $\mathbf{\Gamma}_{0,L}$ and $\mathbf{\Gamma}_{1,L}$ containing only the selected L out of N columns of $\mathbf{\Gamma}_0$ and $\mathbf{\Gamma}_1$. These new matrices play a similar role to the selection matrices in each of the previous CB-DOA algorithms, leading to an implementation of the so-called DFT-beamspace real CB-DOA algorithm as follows. Consider first the transformed autocovariance matrix

$$\mathbf{R}_{00} = \mathbf{\Gamma}_{0,L} \mathbf{Y}_{RI} \mathbf{\Gamma}_{0,L}^{\mathrm{T}}. \tag{43}$$

An EVD is performed on $(\mathbf{R}_{00} - \sigma_n^2 \mathbf{I}_L)$, that is

$$\mathrm{EVD}(\mathbf{R}_{00} - \sigma_n^2 \mathbf{I}_L) = \mathbf{U} \mathbf{\Sigma} \mathbf{U}^{\mathrm{H}}. \tag{44}$$

The M largest eigenvalues of $\mathbf{R}_{00}$ are grouped in $\mathbf{\Sigma}_s$ and their associated eigenvectors in the columns of $\mathbf{U}_s$, allowing us to define $\mathbf{F} = (\mathbf{\Sigma}_s^{1/2})^{-1} \mathbf{U}_s^{\mathrm{H}}$, as before. Applying $\mathbf{F}$ to both sides of $(\mathbf{\Gamma}_{1,L} \mathbf{Y}_{RI} \mathbf{\Gamma}_{0,L}^{\mathrm{T}} - \sigma_n^2 \mathbf{I}_L)$ leads to

$$\begin{aligned} \mathbf{\Upsilon} &= \mathbf{F}(\mathbf{\Gamma}_{1,L} \mathbf{Y}_{RI} \mathbf{\Gamma}_{0,L}^{\mathrm{T}} - \sigma_n^2 \mathbf{I}_L) \mathbf{F}^{\mathrm{H}} \\ &= \mathbf{F} \mathbf{\Gamma}_{0,L} \mathbf{W}_{L,b}^{\mathrm{H}} \mathbf{A} \mathbf{T} (\mathbf{S} \mathbf{\Omega} \mathbf{S}^{\mathrm{H}}) \mathbf{T}^{\mathrm{H}} \mathbf{A}^{\mathrm{H}} \mathbf{W}_{L,b} \mathbf{\Gamma}_{0,L}^{\mathrm{H}} \mathbf{F}^{\mathrm{H}} \end{aligned} \tag{45}$$

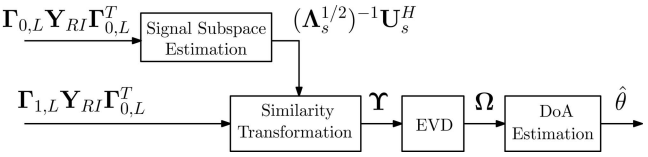

Fig. 4. Block diagram for proposed DFT-beamspace real CB-DOA algorithm.

where $\mathbf{T}$ is a full-rank matrix representing a rotational incertainty in the signal subspace estimation. Therefore, the EVD of $\mathbf{\Upsilon}$ provides matrix $\mathbf{\Omega}$ as in (37):

$$\mathbf{\Omega} = \mathrm{diag}\left(\tan\frac{\omega \sin\theta_0}{2c}, \tan\frac{\omega \sin\theta_1}{2c}, \ldots, \tan\frac{\omega \sin\theta_{M-1}}{2c}\right) \tag{46}$$

and subsequently the DOA estimates $\hat{\theta}_m$, as summarized in Fig. 4.

V. MSE ANALYSIS

In this section an MSE analysis for the elementspace CB-DOA algorithm is proposed in Section VA. In Section VB, this analysis is extended to the DFT-beamspace real CB-DOA algorithm, whose performance is also assessed by the associated Cramer-Rao lower bound (CRLB), as provided in Section VC.

A. MSE Analytic Expression for CB-DOA Methods

Consider the MSE on the DOA estimation defined as

$$\mathrm{MSE}(\hat{\theta}_m, \theta_m) = E[|\Delta\theta_m|^2] = E[|\theta_m - \hat{\theta}_m|^2] \tag{47}$$

where notation Δx designates an estimate error for variable x. As demonstrated in [14], the estimation

MSE for θ_m and ϕ_m are related by

$$E[|\Delta\theta_m|^2] = \left(\frac{1}{\omega\cos\hat{\theta}_m}\right)^2 \frac{E[|\Delta\phi_m|^2]}{2}. \quad (48)$$

Using this relationship, we derive an MSE expression for θ_m using some MSE expression for ϕ_m.

For that purpose, consider the auxiliary matrices $\mathbf{U}_{s0} = \mathbf{J}_0^{P,N}\mathbf{U}_s$ and $\mathbf{U}_{s1} = \mathbf{J}_1^{P,N}\mathbf{U}_s$. From (12), matrix $\mathbf{\Psi}$ provides a rotational invariance property for $\mathbf{U}_X$ of the form $\mathbf{U}_{s0}\mathbf{\Psi} = \mathbf{U}_{s1}$. Therefore, one may write that

$$(\mathbf{U}_{s0} + \mathbf{\Delta U}_{s0})(\mathbf{\Psi} + \mathbf{\Delta\Psi}) = \mathbf{U}_{s1} + \mathbf{\Delta U}_{s1} \quad (49)$$

in such a way that, by considering $\mathbf{\Delta U}_{s0}\mathbf{\Delta\Psi} \approx \mathbf{0}$, one gets

$$\mathbf{\Delta\Psi} = \mathbf{U}_{s0}^{+}(\mathbf{\Delta U}_{s1} - \mathbf{\Delta U}_{s0}\mathbf{\Psi}) \quad (50)$$

where the superscript $^+$ denotes the pseudoinverse operation.

By representing the eigenvalue ϕ_m and its corresponding eigenvector $\mathbf{r}_m$ extracted from matrix $\mathbf{\Delta\Psi}$, a first-order approximation for the expression of $\Delta\phi_m$ is given by

$$\Delta\phi_m = \mathbf{r}_m^{\mathrm{H}}(\mathbf{\Delta\Psi})\mathbf{r}_m. \quad (51)$$

Hence, from (53), (54), and (50), as well as the definition of eigenvalue/eigenvector, one has that

$$\begin{aligned}\Delta\phi_m &= \mathbf{r}_m^{\mathrm{H}}\mathbf{U}_{s0}^{+}(\mathbf{\Delta U}_{s1} - \phi_m\mathbf{\Delta U}_{s0})\mathbf{r}_m \\ &= \mathbf{r}_m^{\mathrm{H}}\mathbf{U}_{s0}^{+}\mathbf{D}_m\mathbf{\Delta U}_X\mathbf{r}_m \end{aligned} \quad (52)$$

with $\mathbf{D}_m = (\mathbf{J}_1^{P,N} - \phi_m\mathbf{J}_0^{P,N})$ and $\mathbf{U}_X$ such that

$$\mathbf{U}_{s0} = \mathbf{J}_0^{P,N}\mathbf{U}_X \quad (53)$$

$$\mathbf{U}_{s1} = \mathbf{J}_1^{P,N}\mathbf{U}_X. \quad (54)$$

Therefore, we may write that

$$E[|\Delta\phi_m|^2] = \mathbf{r}_m^{\mathrm{H}}\mathbf{U}_{s0}^{+}\left(\sum_{j=1}^{M}|\mathbf{r}_j|^2\right)\mathbf{D}_m^{\mathrm{H}}\mathbf{R}_{\Delta u}\mathbf{D}_m(\mathbf{U}_{s0}^{+})^{\mathrm{H}}\mathbf{r}_m \quad (55)$$

where $\mathbf{R}_{\Delta u} = E[\mathbf{\Delta u}_m\mathbf{\Delta u}_n^{\mathrm{H}}]$ is given by

$$\mathbf{R}_{\Delta u} = \frac{\psi_m}{N}\sum_{\substack{k=1\\k\neq m}}\frac{\lambda_m}{(\lambda_k-\lambda_m)^2}\mathbf{u}_k\mathbf{u}_k^{\mathrm{H}}\delta(m-n) \quad (56)$$

in which λ_m^2 represents the mth generalized eigenvalue of $\mathbf{R}_{x00}$, as defined in (20) and $\delta(\cdot)$ denotes the Kronecker's impulse.

The substitution of (55) and (56) into (48) provides an expression for estimating the MSE for θ_m,

$$\begin{aligned}E[|\Delta\theta_m|^2] = &\left(\frac{1}{\omega\cos\hat{\theta}_m}\right)^2\left(\frac{\psi_m}{2N}\right)\mathbf{r}_m^{\mathrm{H}}\mathbf{U}_{s0}^{+}\left(\sum_{j=1}^{M}|\mathbf{r}_j|^2\right)\mathbf{D}_m^{\mathrm{H}} \\ &\times\mathbf{U}_\delta\mathbf{D}_m(\mathbf{U}_{s0}^{+})^{\mathrm{H}}\mathbf{r}_m \end{aligned} \quad (57)$$

where

$$\mathbf{U}_\delta = \left(\sum_{\substack{k=1\\k\neq m}}\frac{\lambda_m}{(\lambda_k-\lambda_m)^2}\mathbf{u}_k\mathbf{u}_k^{\mathrm{H}}\delta(m-n)\right). \quad (58)$$

B. Extension to DFT-Beamspace Real CB-DOA

In [14] one verifies that both the elementspace and beamspace versions of ESPRIT present similar MSE performance when referring to (57), with the only difference being the definition of $\mathbf{D}_m = (\mathbf{J}_1^{P,N} - \phi_m^*\mathbf{J}_0^{P,N})$. The same extension can therefore be inferred to the CB-DOA framework, allowing us to associate the above MSE analysis to any CB-DOA variation seen before. For the DFT-beamspace real CB-DOA algorithm, however, since the rotation invariance is represented by (40), then (53) and (54) should be modified by replacing $\mathbf{J}_0^{P,N}$ and $\mathbf{J}_1^{P,N}$ with $\mathbf{\Upsilon}_0\mathbf{W}_{L,b}^H$ and $\mathbf{\Upsilon}_1\mathbf{W}_{L,b}^H$, respectively. Then, for this particular algorithm, we have the same MSE expression almost as before with

$$\mathbf{D}_m = \mathbf{\Upsilon}_1\mathbf{W}_{L,b}^H - \phi\mathbf{\Upsilon}_0\mathbf{W}_{L,b}^H. \quad (59)$$

Since $\mathbf{\Upsilon}_0$, $\mathbf{\Upsilon}_1$, and $\mathbf{W}_{L,b}^H$ have unit norm, these matrices do not affect the MSE final expression given in (57).

C. Cramer-Rao Lower Bound

The CRLB is a theoretical MSE limit on the unbiased estimation of a given parameter. When using a receiving ULA and a large amount of data is available, the CRLB for each θ_m can be approximated by [3]

$$\begin{aligned}&\mathrm{CRLB}(\theta_i,\hat{\theta}_i) \\ &\quad= \frac{\sigma_n^2}{2N\sigma_s^2}(\Re((\mathbf{d}_i^{\mathrm{H}}\mathbf{W}^{\mathrm{H}}(\mathbf{I}-\mathbf{W}\mathbf{A}(\mathbf{A}^{\mathrm{H}}\mathbf{A})^{-1}\mathbf{A}^{\mathrm{H}}\mathbf{W}^{\mathrm{H}})\mathbf{W}\mathbf{d}_i)))^{-1}\end{aligned} \quad (60)$$

where σ_s^2 is the mean power for the transmitted signal and

$$\mathbf{d}_i = \frac{d}{d\omega_i}\mathbf{a}_i \quad (61)$$

represents the derivative of each steering array vector $\mathbf{a}_i$. For the DFT-beamspace real CB-DOA algorithm, each ω_i is related to ϕ_i according to (37), while (60) represents a simplification for the original formulation, but $\mathbf{Y}_{RI}$ is considered an identity matrix.

VI. COMPUTATIONAL COMPLEXITY

This section compares the computational complexity of the proposed DFT-beamspace real CB-DOA algorithm to an ESPRIT counterpart introduced in [13], with both algorithms as summarized in Table I.

TABLE I
Short Descriptions of DFT-Beamspace Real Versions of Both ESPRIT and CB-DOA Algorithms

DFT-Beamspace Unitary ESPRIT	DFT-Beamspace Real CB-DOA
$\mathbf{Y}_r = \mathbf{W}_{L,b}^{\mathrm{H}}\mathbf{X}$	$\mathbf{Y}_r = \mathbf{W}_{L,b}^{\mathrm{H}}\mathbf{X}$
$\mathbf{Y}_{RI} = [\Re(\mathbf{Y}_r) \quad \Im(\mathbf{Y}_r)] \begin{bmatrix} (\Re(\mathbf{Y}_r))^{\mathrm{T}} \\ (\Im(\mathbf{Y}_r))^{\mathrm{T}} \end{bmatrix}$	$\mathbf{Y}_{RI} = [\Re(\mathbf{Y}_r) \quad \Im(\mathbf{Y}_r)] \begin{bmatrix} (\Re(\mathbf{Y}_r))^{\mathrm{T}} \\ (\Im(\mathbf{Y}_r))^{\mathrm{T}} \end{bmatrix}$
$[\mathbf{\Sigma}_s, \mathbf{U}_s] = \mathrm{EVD}(\mathbf{Y}_{RI} - \sigma_n^2\mathbf{I}_L)$	$[\mathbf{\Sigma}_s, \mathbf{U}_s] = \mathrm{EVD}(\mathbf{\Gamma}_{0,L}(\mathbf{Y}_{RI} - \sigma_n^2\mathbf{I}_L)\mathbf{\Gamma}_{0,L}^{\mathrm{T}})$
$\mathbf{E}_0 = \mathbf{\Gamma}_{0,L}\mathbf{U}_s$	$\mathbf{F} = (\mathbf{\Sigma}_s^{1/2})^{-1}\mathbf{U}_s^{\mathrm{H}}$
$\mathbf{E}_1 = \mathbf{\Gamma}_{1,L}\mathbf{U}_s$	$\mathbf{R}_{10} = \mathbf{\Gamma}_{1,L}\mathbf{Y}_{RI}\mathbf{\Gamma}_{0,L}^{\mathrm{T}}$
$\mathbf{E}_a = \begin{bmatrix} \mathbf{E}_0^{\mathrm{T}} \\ \mathbf{E}_1^{\mathrm{T}} \end{bmatrix} [\mathbf{E}_0 \quad \mathbf{E}_1]$	
$[\mathbf{E}, \mathbf{\Lambda}] = \mathrm{EVD}(\mathbf{E}_a)$	
$\mathbf{E}_{01} = \mathbf{J}_0^{M,2M}\mathbf{E}(\mathbf{J}_0^{M,2M})^{\mathrm{T}}$	
$\mathbf{E}_{11} = \mathbf{J}_{1,M}\mathbf{E}\mathbf{J}_{1,M}^{\mathrm{T}}$	
$\mathbf{\Upsilon} = -\mathbf{E}_{01}\mathbf{E}_{11}^{-1}$	$\mathbf{\Upsilon} = \mathbf{F}(\mathbf{R}_{10} - \sigma_n^2\mathbf{I}_M)\mathbf{F}^{\mathrm{H}}$
$[\mathbf{\Omega}] = \mathrm{EVD}(\mathbf{\Upsilon})$	$[\mathbf{\Omega}] = \mathrm{EVD}(\mathbf{\Upsilon})$
$\hat{\mathbf{\Theta}} = \arcsin\left(\frac{2c}{\omega}\arctan\mathbf{\Omega}\right)$	$\hat{\mathbf{\Theta}} = \arcsin\left(\frac{2c}{\omega}\arctan\mathbf{\Omega}\right)$

From Table I a summary of all operations required for both algorithms can be determined, as presented in Table II, along with the corresponding computational complexity, as provided in [7]. In this table, multiplications involving the banded matrices $\mathbf{\Gamma}_{0,L}$ and $\mathbf{\Gamma}_{1,L}$ present lower complexity, since these matrices have only 2 out of L non-zero entries per row.

If only the dominant terms in Table II are considered for a simplified analysis, an approximate expression for the reduction in the computational complexity Compl(·) for the two algorithms is given by

$$\frac{\mathrm{Compl(CB\text{-}DOA)}}{\mathrm{Compl(ESPRIT)}} = \frac{LN^2 + L^2N + 25M^3}{LN^2 + 2L^2N + 25.6M^3}. \quad (62)$$

For the simplest case of $M = 1$ and $N = L = 2$, the reduction in complexity is always greater than 20%. Larger numbers of receiving antennas N and/or beamspace dimension L reduce the computational complexity even further, as verified in the communications scenarios considered in the following section.

VII. SIMULATIONS

In this section some simulations are provided in order to evaluate the MSE performance for the DFT-beamspace real versions of both the ESPRIT and CB-DOA algorithms. In each situation the MSE is averaged over 200 Monte Carlo runs of 9000 data snapshots each, for a wide range of signal-to-noise ratios (SNRs). For comparison purposes, in each case we also include the CRLB, the theoretical MSE derived in Section V, and the MSE for the maximum likelihood (ML) estimator characterized by [2]

$$\theta_{\mathrm{ML}} = \arg\min_{\theta}\left\{\det\left[\mathbf{P}_A\mathbf{R}_X\mathbf{P}_A + \frac{1}{N}\mathrm{tr}(\mathbf{P}_A^{\perp}\mathbf{R}_X)\mathbf{P}_A^{\perp}\right]\right\} \quad (63)$$

where $\mathbf{P}_A = \mathbf{A}_{\mathrm{ext}}(\mathbf{A}_{\mathrm{ext}}^H\mathbf{A}_{\mathrm{ext}})\mathbf{A}_{\mathrm{ext}}^H$ is the projection matrix onto the columns of the extended array manifold matrix

$$\mathbf{A}_{\mathrm{ext}} = \begin{bmatrix} \mathbf{A} \\ \mathbf{A}\mathbf{\Phi} \end{bmatrix}. \quad (64)$$

Since some of the structures are used with beamspace projections, we may also utilize the beamspace ML estimator given by [2]

$$\theta_{\mathrm{beam\,ML}} = \arg\min_{\theta}\left\{\det\left[\mathbf{P}_B\mathbf{R}_X\mathbf{P}_B + \frac{1}{N}\mathrm{tr}(\mathbf{P}_B^{\perp}\mathbf{R}_X)\mathbf{P}_A^{\perp}\right]\right\} \quad (65)$$

where $\mathbf{P}_B = \mathbf{W}_{L,b}^H\mathbf{P}_A\mathbf{W}_{L,b}$ corresponds to a new projection matrix.

The first scenario comprises $M = 1$ source at 7°, $N = 13$ receiving antennas, and a beamspace with

TABLE II
Number of Matrix Operations Required by DFT-Beamspace Unitary/Real Versions of ESPRIT and CB-DOA Algorithms

Matrix Operation [7]	DFT-Beamspace Unitary ESPRIT		DFT-Beamspace Real CB-DOA	
	#	Flops	#	Flops
EVD	1	$25M^3$	1	$25M^3$
Hermitian EVD	2	$L^2 + 4M^2$	1	$(L-1)^2$
Inversion	1	$(2/3)M^3$	—	—
Diag. Inversion	—	—	1	M
Multiplication	8	$LN^2 + M^3 + 4M^2(L-1) + 2L^2N$	6	$LN^2 + L^2N + M(L-1)^2 + M^2(L-1)$
Banded Multiplication	2	$4(L-1)M$	4	$4L(L-1) + 4L^2$
Dominant Terms		$LN^2 + 2L^2N + 25.6M^3$		$LN^2 + L^2N + 25M^3$

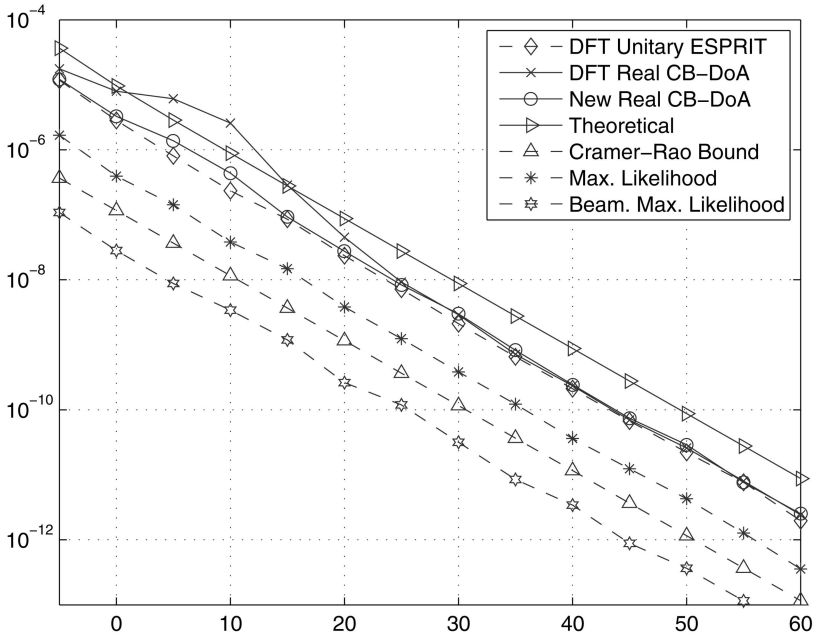

Fig. 5. Simulated MSE as function of SNR, for $M = 1$ source, $N = 13$ antennas, beamspace with dimension $L = 9$.

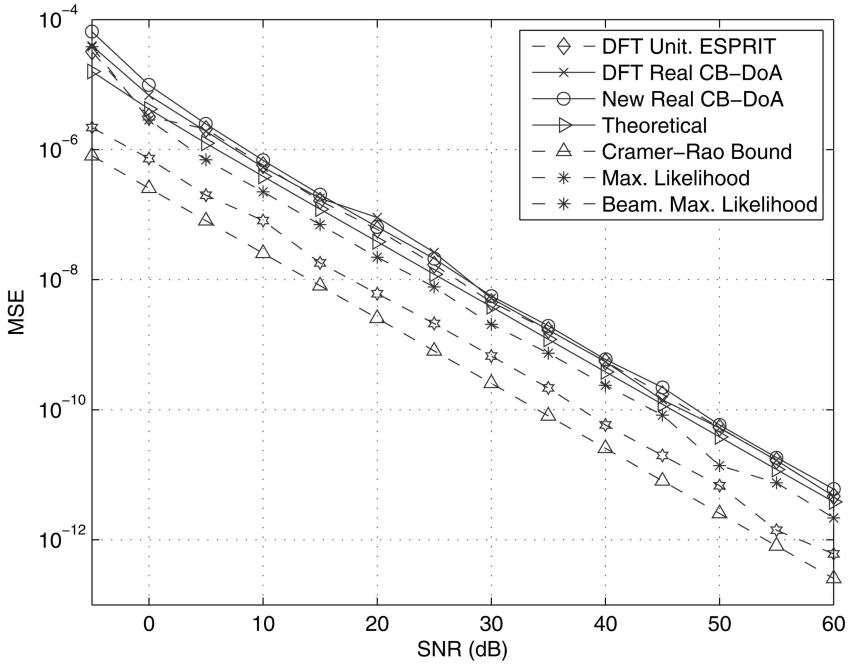

Fig. 6. Simulated MSE as function of SNR, for $M = 2$ sources, $N = 15$ antennas, beamspace with dimension $L = 12$.

dimension $L = 9$. According to the analysis presented in Section VI, in this setup, the DFT-beamspace real CB-DOA requires at least 20% less flops than its ESPRIT counterpart, while presenting similar MSE results, as verified in Fig. 5. From this figure, one also observes how the theoretical MSE analysis complies reasonably well with the simulated CB-DOA algorithm, whereas the CRLB and ML estimator, respectively, provide theoretical and practical top-notch performances, in spite of the prohibitive computational cost.

In Fig. 6 simulations are performed for $M = 2$ sources, located at angles 2° and 7°, and $N = 15$ receiving antennas, and beamspace of size $L = 12$. Once again, the DFT-beamspace real CB-DOA algorithm presents a similar MSE performance to the DFT-beamspace unitary ESPRIT, while demanding around 30% less flops, as predicted in Section VI. In this scenario the theoretical MSE analysis models accurately the CB-DOA algorithm, whose performance approaches the ML algorithm, due to the larger values of N and L.

Qualitative results depicted in Figs. 5 and 6 were verified for several communications setups, with distinct values of L, M, or N. Higher values of L and N lead to greater reduction in the computational complexity when using the CB-DOA framework as compared with the ESPRIT algorithm.

VIII. CONCLUSION

This article proposes a new CB-DOA algorithm, simultaneously incorporating beamspace and real-only-operation projections, which significantly reduce the overall computational complexity in comparison to the similar ESPRIT scheme. In comparison to previous CB-DOA algorithms, the so-called DFT-beamspace real CB-DOA requires less data elements than the real CB-DOA scheme and processes smaller data structures than the beamspace CB-DOA algorithm.

In comparison to DFT-beamspace unitary ESPRIT, the proposed algorithm presents a similar MSE performance and reduced computational complexity, as verified by theoretical and simulation experiments. Simplification starts at the 20% level and increases even further for larger numbers of receiving antennas or beamspace dimensions. Other contributions of this article include MSE analysis for the CB-DOA family of algorithms and a new version for the real CB-DOA algorithm, whose formulation made it possible to derive the proposed DFT-beamspace real CB-DOA algorithm.

REFERENCES

[1] Godara, L. C.
Applications of antenna arrays to mobile communications. I. Performance improvement, feasibility and system considerations.
Proceedings of the IEEE, **85**, 7 (July 1997), 1031–1060.

[2] Van Trees, H.
Detection, Estimation and Modulation Theory, Part IV: Optimum Array Processing.
Hoboken, NJ: Wiley, 2002.

[3] Stoica, P. and Nehorai, A.
MUSIC, maximum likelihood and Crámer-Rao bound.
IEEE Transactions on Acoustics, Speech and Signal Processing, **37**, 5 (May 1989), 720–741.

[4] Roy, R. H. and Kailath, T.
ESPRIT—Estimation of parameters via rotational invariance techniques.
IEEE Transactions on Acoustics, Speech and Signal Processing, **37**, 7 (July 1989), 984–995.

[5] Ma, Y., et al.
Dimensionality reduction via subspace and submanifold learning.
IEEE Signal Processing Magazine, **28**, 2 (Mar. 2011), 14–15, 126.

[6] Ferreira, T. N., Netto, S. L., and Diniz, P. S. R.
Low complexity covariance-based DOA estimation algorithm.
In *Proceedings of the 15th European Signal Processing Conference*, Poznan, Poland, Sept. 2007, 100–104.

[7] Golub, G. and Van Loan, C.
Matrix Computations (3rd ed.).
Baltimore, MD: Johns Hopkins University Press, 1996.

[8] Almidfa, K., Tsoulos, G., and Nix, A.
Performance analysis of ESPRIT, TLS-ESPRIT and unitary ESPRIT algorithms for DOA estimation in a WCDMA mobile system.
In *Proceedings of the International Conference on 3G Mobile Communication Technologies*, Mar. 2000, 200–203.

[9] Tong, L., Xu, G., and Kailath, T.
Blind identification and equalization based on second-order statistics: A time-domain approach.
IEEE Transactions on Information Theory, **40**, 2 (Mar. 1994), 340–349.

[10] Xu, G., et al.
Beamspace ESPRIT.
IEEE Transactions on Signal Processing, **42**, 2 (Feb. 1994), 349–356.

[11] Ferreira, T. N., Netto, S. L., and Diniz, P. S. R.
Beamspace covariance-based DOA estimation.
In *Proceedings of the IEEE Workshop on Signal Processing Advances in Wireless Communications*, Recife, Brazil, July 2008, 136–140.

[12] Ferreira, T. N., Netto, S. L., and Diniz, P. S. R.
Covariance-based direction-of-arrival estimation with real structures.
IEEE Signal Processing Letters, **15** (Dec. 2008), 757–760.

[13] Zoltowski, M. D., Haardt, M., and Mathews, C. P.
Closed-form 2-D angle estimation with rectangular arrays in element space or beamspace via unitary ESPRIT.
IEEE Transactions on Signal Processing, **44** (Feb. 1996), 316–328.

[14] Rao, B. D. and Hari, K. V. S.
Performance analysis of ESPRIT and TAM in determining the direction of arrival of plane waves in noise.
IEEE Transactions on Acoustics, Speech and Signal Processing, **37** (Dec. 1989), 1990–1995.

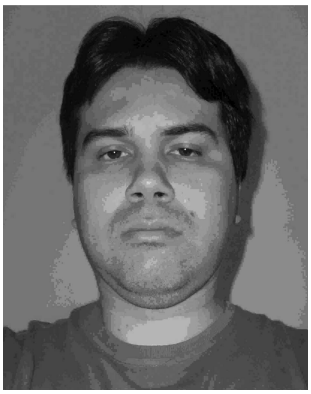

Tadeu Ferreira (M'10) was born in Rio de Janeiro, Brazil in 1978. He majored in electronics engineering at UFRJ (Brazil) in 2003, received M.Sc. degree from COPPE/UFRJ in 2005, and D.Sc. degree from COPPE/UFRJ in 2009.

He worked as a technical high-school teacher at CEFET/RJ Uned Nova Iguaçu in 2010. He has been an adjunct professor at Fluminense Federal University (UFF) since November 2010.

Sergio L. Netto (SM'04) was born in Rio de Janeiro, Brazil. He received the B.Sc. degree (cum laude) from the Federal University of Rio de Janeiro (UFRJ), Brazil, in 1991, the M.Sc. degree from COPPE/UFRJ in 1992, and the Ph.D. degree from the University of Victoria, BC, Canada, in 1996, all in electrical engineering.

Since 1997 he has been an associate professor with the Department of Electronics and Computer Engineering, at Poli/UFRJ, and since 1998 with the Program of Electrical Engineering, at COPPE/UFRJ. His research interests lie in the areas of digital signal processing, and speech processing (coding and quality evaluation).

Dr. Netto is the coauthor (with P. S. R. Diniz and E. A. B. da Silva) of *Digital Signal Processing: System Analysis and Design* 2nd ed. (Cambridge University Press, 2010).

Paulo S. R. Diniz (F'00) was born in Niterói, Brazil. He received the Electronics Eng. degree (cum laude) from the Federal University of Rio de Janeiro (UFRJ) in 1978, the M.Sc. degree from COPPE/UFRJ in 1981, and the Ph.D. from Concordia University, Montreal, P.Q., Canada, in 1984, all in electrical engineering.

Since 1979 he has been with the Department of Electronic Engineering (the undergraduate department), UFRJ. He has also been with the Program of Electrical Engineering (the graduate studies department), COPPE/UFRJ, since 1984, where he is presently a professor. He served as Undergraduate Course Coordinator and as Chairman of the Graduate Department. He is one of the three senior researchers and coordinators of the National Excellence Center in Signal Processing. He has also received the Rio de Janeiro State Scientist award, from the Governor of Rio de Janeiro state.

From January 1991 to July 1992, he was a visiting research associate in the Department of Electrical and Computer Engineering, University of Victoria, Victoria, B.C., Canada. He also holds a Docent position at Helsinki University of Technology. From January 2002 to June 2002, he was a Melchor Chair Professor in the Department of Electrical Engineering, University of Notre Dame, Notre Dame, IN. His teaching and research interests are in analog and digital signal processing, adaptive signal processing, digital communications, wireless communications, multirate systems, stochastic processes, and electronic circuits.

He has published several refereed papers in some of the areas of his research interests and wrote the books *ADAPTIVE FILTERING: Algorithms and Practical Implementation* 3rd ed. (Springer, 2008), and *DIGITAL SIGNAL PROCESSING: System Analysis and Design* (Cambridge University Press, 2002) (with E. A. B. da Silva and S. L. Netto).

Dr. Diniz has served as the Technical Program Chair of the 1995 MWSCAS held in Rio de Janeiro, Brazil. He is the General Cochair of ISCAS2011, and Technical Program Cochair of SPAWC2008. He has been on the technical committee of several international conferences including ISCAS, ICECS, EUSIPCO, and MWSCAS. He has served as vice president for region 9 of the IEEE Circuits and Systems Society and as Chairman of the DSP Technical Committee of the same Society. He has served as associate editor for the following journals: *IEEE Transactions on Circuits and Systems II: Analog and Digital Signal Processing* from 1996 to 1999, *IEEE Transactions on Signal Processing* from 1999 to 2002, and *Circuits, Systems and Signal Processing Journal* from 1998 to 2002. He was a Distinguished Lecturer of the IEEE Circuits and Systems Society for the year 2000 to 2001. In 2004 he served as Distinguished Lecturer of the IEEE Signal Processing Society and received the 2004 Education Award of the IEEE Circuits and Systems Society.